

# The energy dependence on the density depression parameter

M. Ismail<sup>1</sup>, A. Y. Ellithi<sup>1</sup>, M. M. Botros<sup>1</sup>, Walaa M. T. Abd-Alaa<sup>2</sup>

<sup>1</sup> Department of physics, Faculty of Science, Cairo University, Giza, Egypt.

<sup>2</sup> Department of physics, Faculty of Engineering 6th October University.

**Abstract-** A semi-microscopic approach based on Skyrme energy density functional is used to study the effect of the depression parameter ( $\beta$ ) of the density distribution of protons and neutrons on the total energy of nuclei with proton number  $Z = 18, 114, 116$  and  $120$ . For each element, two isotopes are considered. The variation of the contribution of the total energy parts with the depression parameter is studied. For super heavy nuclei, the variation of the lowest total energy curve with  $\beta$  has a shallow minimum, which occurs at negative value of  $\beta$ , suggesting that, these nuclei prefer large values of density at of their centers, these nuclei gain about  $15$  MeV in their binding energies within the  $\beta$  range considered. For the lightest Ar nucleus, the minimum is clear and occurs at positive value of  $\beta$

**Keywords-** Binding energy; Energy density function; Density depression.

## 1. INTRODUCTION:

The synthesis of super heavy elements (SHE'S) was and still an outstanding research object [1], exploration of the domain of superheavy nuclei (SHN) has been pursued for a long time and the limits on stability and feasibility of creating these heavy nuclei have been under test [1]. The progress in experimental techniques has drawn the attention and opened up the field once again for further improvements in theoretical studies and predictions for superheavy nuclei. Physics of the structure of these nuclei has been very intense in recent years [2]. Microscopic calculations show that some of light and SHN has central depression in their density distributions. As an example, as an extreme case of central depressed nuclear density, the nuclear bubble has attracted great attention [3]. Self consistent microscopic calculations find a central depression in the nuclear density distribution which generates a wine-bottle shaped nucleonic potential, its magic numbers differ from flat bottom potentials.

In this paper, we deal with a semi-microscopic, but not self- consistent model, which uses the Skyrme nucleon-nucleon interaction in the semi-classical extended Thomas-Fermi approach (ETF) to obtain the macroscopic energy part which depends on nuclear density in the presence of the depression parameter. In the present calculations, we neglect the shell plus pairing corrections due to the complexity of their calculations in the presence depression parameters. The Skyrme energy density functional is applied to make the study of the total energy, for a series of nuclei (Light and superheavy), in presence of the depression parameter in the density distribution of protons and neutrons. This method has the advantage of being much faster and giving more information than the Hartree-Fock (HF) calculations carried out to date.

## 2. THEORETICAL FRAMEWORK

In the framework of ETF approach together with a Skyrme effective nucleon - nucleon interaction, the total energy density functional of a nucleus can be derived systematically. This energy density functional is widely used in studying the nuclear ground state properties [4].

Thus, we take the Skyrme-Hartree-Fock (Skyrme-HF) formalism of the energy density functional [4] and we calculate the total energy in the presence of the depression parameter  $\beta$  in the density distributions of protons and neutrons. In this approach, the total energy of a nucleus is

$$E = \int H(r) d^3r \quad (1)$$

The energy density functional  $H(r)$  includes the kinetic, nuclear and Coulomb interaction energy parts.

$$H(\vec{r}) = \frac{\hbar^2}{2m} [\tau_p(\vec{r}) + \tau_n(\vec{r})] + H_{\text{Sky}}(\vec{r}) + H_{\text{Coul}}(\vec{r}) \quad (2)$$

For the kinetic energy part, ETF approach including all terms up to second order in the spatial derivatives, is applied as [6], with the effective-mass form factor.

$$f_i(\vec{r}) = 1 + \frac{2m}{\hbar^2} \left( \frac{3t_1 + 5t_2}{16} + \frac{t_2 x_2}{4} \right) \rho_i(\vec{r}) \quad (i = n, p) \quad (3)$$

where  $t_1$ ,  $t_2$  and  $x_2$  are the Skyrme-force parameters.  $\rho_i(\vec{r})$  denotes the proton or neutron density of the nucleus and it is given by the three-parameter Fermi (3PF) distribution which takes the form [7]

$$\rho_i(\vec{r}) = \rho_i^0 \frac{\left\{ \alpha + \beta_i \left( \frac{r}{R_i^0} \right)^2 \right\}}{1 + e^{\frac{r - R_i^0}{a}}} \quad (i = n, p) \quad (4)$$

such that, the total nuclear density  $\rho(r) = \rho_p(r) + \rho_n(r)$ ,  $\rho_i^0$  is the normalization constant for protons ( $i=p$ ) and neutrons ( $i=n$ ),  $\alpha$ , is a constant ( $\alpha = 0.9$ ).  $\beta$  is the depression parameter and we take its range as (-0.2 to 0.6). The greater values of  $\beta_i$  is, the more depressed central density.  $R_i^0$  is the density radius parameter of protons or neutrons such that:

$$R_p^0 = 1.28 A^{\frac{1}{3}} - 0.76 + 0.8A^{-\frac{1}{3}} \quad (5)$$

$$R_n^0 = R_p^0 + \Delta R \quad (6)$$

where  $A$  is the mass number,  $\Delta R = 0.2$  fm is the neutrons skin thickness which is adjusted to fit the experimental data. The **kinetic energy** densities  $\tau_i(r)$  are given by

$$\begin{aligned} \tau_i(r) = & \frac{3}{5} (3\pi^2)^{\frac{2}{3}} \rho_i^{\frac{5}{3}} + \frac{1}{36} \frac{(\nabla \rho_i)^2}{\rho_i} \\ & + \frac{1}{3} \Delta \rho_i + \frac{1}{6} \frac{\nabla \rho_i \nabla f_i + \rho_i \Delta f_i}{f_i} \\ & - \frac{1}{12} \rho_i \left( \frac{\nabla f_i}{f_i} \right)^2 + \frac{1}{2} \rho_i \left( \frac{2m \omega_0 \nabla(\rho + \rho_i)}{2 \hbar^2 f_i} \right)^2 \end{aligned} \quad (7)$$

where  $\omega_0$  denotes the strength of the Skyrme spin-orbit interactions, while  $\rho = \rho_p + \rho_n$ .

The *nuclear part* of the Skyrme–Hamiltonian density  $H_{\text{Sky}}(\vec{r})$  reads, [8]

$$\begin{aligned} \mathcal{H}_{\text{sky}}(\vec{r}) = & \frac{t_0}{2} \left[ \left( 1 + \frac{1}{2} \chi_0 \right) \rho^2 - \left( \chi_0 + \frac{1}{2} \right) (\rho_p^2 + \rho_n^2) \right] \\ & + \frac{1}{12} t_3 \rho^\gamma \left[ \left( 1 + \frac{1}{2} \chi_3 \right) \rho^2 - \left( \chi_3 + \frac{1}{2} \right) (\rho_p^2 + \rho_n^2) \right] \\ & + \frac{1}{4} \left[ t_1 \left( 1 + \frac{1}{2} \chi_1 \right) + t_2 \left( 1 + \frac{1}{2} \chi_2 \right) \right] \tau \rho \\ & + \frac{1}{4} \left[ t_2 \left( \chi_2 + \frac{1}{2} \right) - t_1 \left( \chi_1 + \frac{1}{2} \right) \right] (\tau_p \rho_p + \tau_n \rho_n) \\ & + \frac{1}{16} \left[ 3t_1 \left( 1 + \frac{1}{2} \chi_1 \right) - t_2 \left( 1 + \frac{1}{2} \chi_2 \right) \right] (\nabla \rho)^2 \\ & - \frac{1}{16} \left[ 3t_1 \left( \chi_1 + \frac{1}{2} \right) + t_2 \left( \chi_2 + \frac{1}{2} \right) \right] \left( (\nabla \rho_n)^2 + (\nabla \rho_p)^2 \right) \\ & - \frac{\omega_0^2}{4} \frac{2m}{\hbar^2} \left[ \frac{\rho_p}{f_p} (2\nabla \rho_p + \nabla \rho_n)^2 + \frac{\rho_n}{f_n} (2\nabla \rho_n + \nabla \rho_p)^2 \right] \end{aligned} \quad (8)$$

where  $t_0, t_1, t_2, t_3, \chi_0, \chi_1, \chi_2, \chi_3, \gamma, \omega_0$  are the Skyrme-force parameters. The use of effective Skyrme forces in investigating the properties of nuclear systems facilitates the numerical calculations considerably. For the Skyrme forces, there are several sets of parameters usually adjusted to the different mass regions or different observables. The frequently used sets are, SK III [9], SKM\* [10], SKP [11] or SLY6 [12]. The total binding energy of nuclei is calculated in the present paper using SKM\* set of parameters, since it is very successful for describing the bulk and

surface properties of nuclei. It is a well known fact that, an ETF calculation with a reasonable effective interaction reproduces the experimental binding energies with a very good accuracy.

Although the correct description of nuclei, one has to add to the nuclear and kinetic energies and the direct and exchange contributions of the Coulomb interaction energy. In our calculations we deal only with the direct part of Coulomb energy in presence of the depression parameters  $\beta$ , [8].

$$E_D^C = \int d\vec{r}_1 \int d\vec{r}_2 v(s) \rho_p(\vec{r}_1) \rho_p(\vec{r}_2) \quad (9)$$

where  $v(s)$  is the Coulomb potential between two protons and  $(s)$  is their separation distance.

### 3. NUMERICAL RESULTS AND DISCUSSION

The total energy composed of three contributions namely, Coulomb energy given by equation (9), kinetic energy and nuclear potential energy given respectively by the equations

$$E_K = \frac{\hbar^2}{2m} \int [\tau_p(\vec{r}) + \tau_n(\vec{r})] d\vec{r} \quad (10)$$

$$E_{pot} = \int H_{Sky}(\vec{r}) d\vec{r} \quad (11)$$

We study the variation of the total energy for a number of nuclei with depression parameter of protons  $\beta_p$  and neutrons  $\beta_n$ . For each nucleus, we deal with two isotopes and take their values as variation parameters to obtain the lowest total energy for each isotope.

#### 3.1 The two isotopes $^{286}\text{Fl}$ and $^{300}\text{Fl}$

The dependence of the total energy,  $E_{total} = E_C + E_K + E_{pot}$ , of  $^{286}\text{Fl}$  on  $\beta_p$  and  $\beta_n$  is presented on figure (1). The minimum value of the lowest energy curve is the binding energy of the nucleus. As  $\beta_n$  or  $\beta_p$  increases from (-0.2 to 0.6), both the Coulomb and kinetic energies are decreasing while the potential energy increases by an amount depends on the value of  $\beta_n$  and  $\beta_p$ . The competition between sum ( $E_k + E_C$ ) and potential energies produce the curves in the figure. The minimum of the lowest energy curve occurs at  $\beta_n = -0.2$  and  $\beta_p = -0.15$  and the binding energy is about -1990 MeV corresponding to about 6.96 MeV per nucleon. The nucleus gains about 15 MeV in its binding energy due to the existence of  $\beta$  parameters.

Figure (2) is the same as figures (1), but for the heavier isotope  $^{300}\text{Fl}$  whose number of neutrons  $N=186$ , exceeds the protons number by a factor 1.63. The figure shows that the lowest value of the total energy occurs at  $\beta_n = -0.2$ ,  $\beta_p = -0.2$  with value -2079 MeV, corresponding to about 6.93 MeV per nucleon. The nucleus gained about 14 MeV in its binding energy due to the existence of depression parameter.

It is interesting to study the variation of the three contributions of total energy with both depression parameter and nuclear radius. Figures (3) show this study for the SHN  $^{300}\text{Fl}$ . For specific value of nuclear radius, both the Coulomb and kinetic energies decrease with increasing  $\beta$  while the Skyrme potential energy increases (become more repulsive) as  $\beta$  increases. When the radius of the nucleus increases the curves representing the Coulomb and kinetic energies are lowered (as shown on figures (3a) and (3b) respectively), while the potential energy lines are raised up (as shown in figure (3c)). The lines representing the Coulomb, kinetic and potential energy variation with  $\beta$  parameter for each value of nuclear radius are almost parallel. Figure (3d) displays the  $\beta$ -variation of the total energy at different values of the radius parameter. As the value of radius increases, the nucleus becomes less bound. It should be noted that for the  $^{300}\text{Fl}$  element the variation of the low total energy curves is too slow and the minimum (if exists) is too shallow. For these curves, the total energy is not sensitive to the  $\beta$  variation.

#### 3.2 The two SHE'S $Z=116$ and $Z=120$ .

Similarly to the previous section, we calculate the total energy curves for the two superheavy isotopes  $^{280}_{116}$  and  $^{300}_{116}$  and the two isotopes  $^{288}_{120}$  and  $^{304}_{120}$ , the results are shown in figures (4) and (5) respectively. We note that for the two isotopes of each element, the variation of  $E_{total}$  with  $\beta$  has no clear minimum, and when it exists it is too shallow. This behavior is the same as for the isotopes of Fl element in the previous section. The lowest energy

curve has minimum occurs at  $(\beta_n, \beta_p) = (-0.2, -0.1)$  for  $^{280}_{116}$ ,  $(-0.2, -0.15)$  for  $^{300}_{116}$ ,  $(-0.2, -0.10)$  for  $^{288}_{120}$  and at  $(-0.2, -0.15)$  for the isotope  $^{304}_{120}$ . The values predicted for binding energies of  $^{280}_{116}$ ,  $^{300}_{116}$ ,  $^{288}_{120}$  and  $^{304}_{120}$  are -1931, -2074, -1955 and -2067 MeV, respectively, corresponding to binding energies per nucleon 6.87, 6.91, 6.79 and 6.80 MeV per nucleon.

### 3.3 The two light isotopes $^{36}_{18}\text{Ar}$ and $^{46}_{18}\text{Ar}$ .

In this section, we consider two isotopes of lighter nucleus *Ar*. Figures (6a) and (6b) show the variation of the total energy of  $^{36}_{18}\text{Ar}$  and  $^{46}_{18}\text{Ar}$  respectively with depression parameter  $\beta_p = \beta_n = \beta$ . The two curves have the same behavior, the difference between one isotope and another is the minimum value of the total energy. The minimum in case of  $^{46}_{18}\text{Ar}$  is not clear as that in the other isotope  $^{36}_{18}\text{Ar}$ . The behavior of the total energy curves for Argon isotopes differs from that of the heavier nuclei considered in the previous sections, the clear minimum value for each curve of *Ar* is located at a positive value of  $\beta$  indicating that the nucleus gains much binding when its density at the center is depressed. For  $^{36}_{18}\text{Ar}$  the minimum occurs at about  $\beta = 0.15$  at its value is -293 MeV corresponding to binding energy per nucleon of -8.1 MeV. For the neutron rich isotope  $^{46}_{18}\text{Ar}$ , the minimum is shallow and located at about  $\beta = 0.47$  and its value is about -368 MeV corresponding to binding energy per nucleon of -8.0 MeV

## 4. SUMMARY AND CONCLUSIONS

We studied the dependence of total energy of a nucleus on the depression parameter  $\beta$  for the superheavy nuclei with atomic number  $Z=114, 116$  and  $120$  and the light nucleus Argon. For each element, we considered two isotopes and showed the variation of different contributions of the total energy (kinetic, Coulomb and potential energy) with the depression parameter of the density distribution. Each energy part is affected by varying the depression parameter. Both Coulomb and kinetic energy contributions decrease with the increase of the value of the parameter  $\beta$ . The nuclear potential contribution behaves inversely with increasing  $\beta$ , i.e. potential energy becomes less attractive with increasing the value of  $\beta$ . This competition between kinetic energy and Coulomb energy from one side and potential from the other side controls the behavior of the total energy curve with  $\beta$  variation; it may have a clear minimum value at a certain value of the parameter  $\beta$ . For superheavy nuclei, the minimum in the total energy curves are always shallow and occur at negative values of  $\beta$  i.e. these nuclei prefer large value of the density at their centers. For the light  $^{30,46}_{18}\text{Ar}$  nucleus, the minimum is clear and occurs at positive value of depression parameter  $\beta$ .

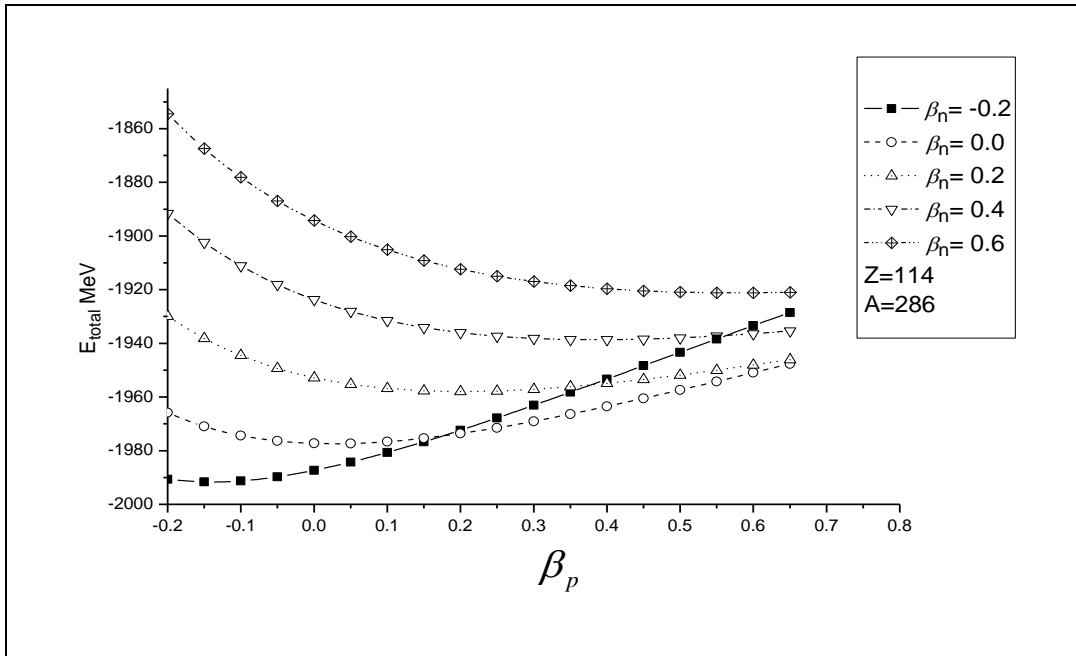


Figure (1): The variation of the total energy (sum of kinetic, nuclear and Coulomb energies) of SHE  $^{286}\text{Fl}$ , with proton depression parameter  $\beta_p$  at 5-values of neutron depression parameter  $\beta_n$ .

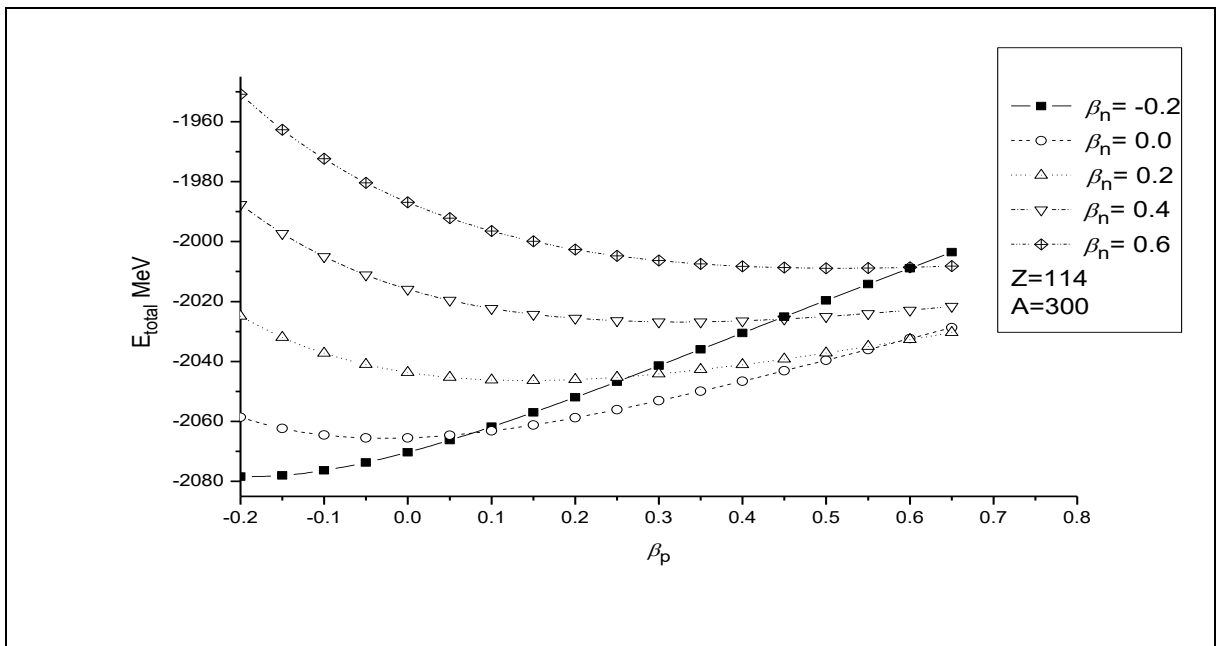


Figure (2): is the same as Figure (1), but for the heavier isotope  $^{300}\text{Fl}$ .

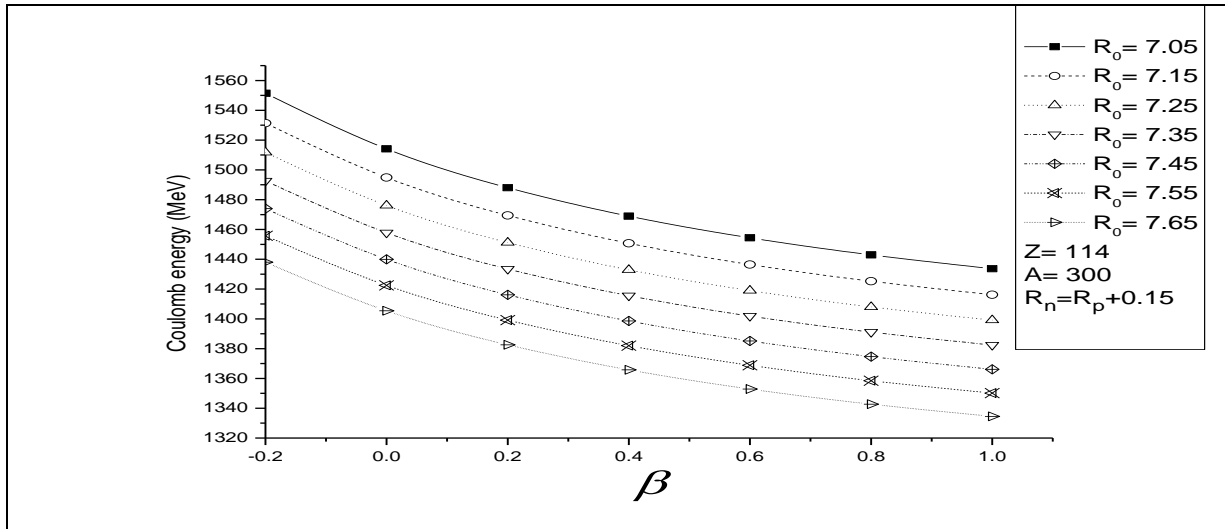


Figure 3(a): The variation of Coulomb energy of <sup>300</sup>Fl nucleus with depression parameter  $\beta$ .

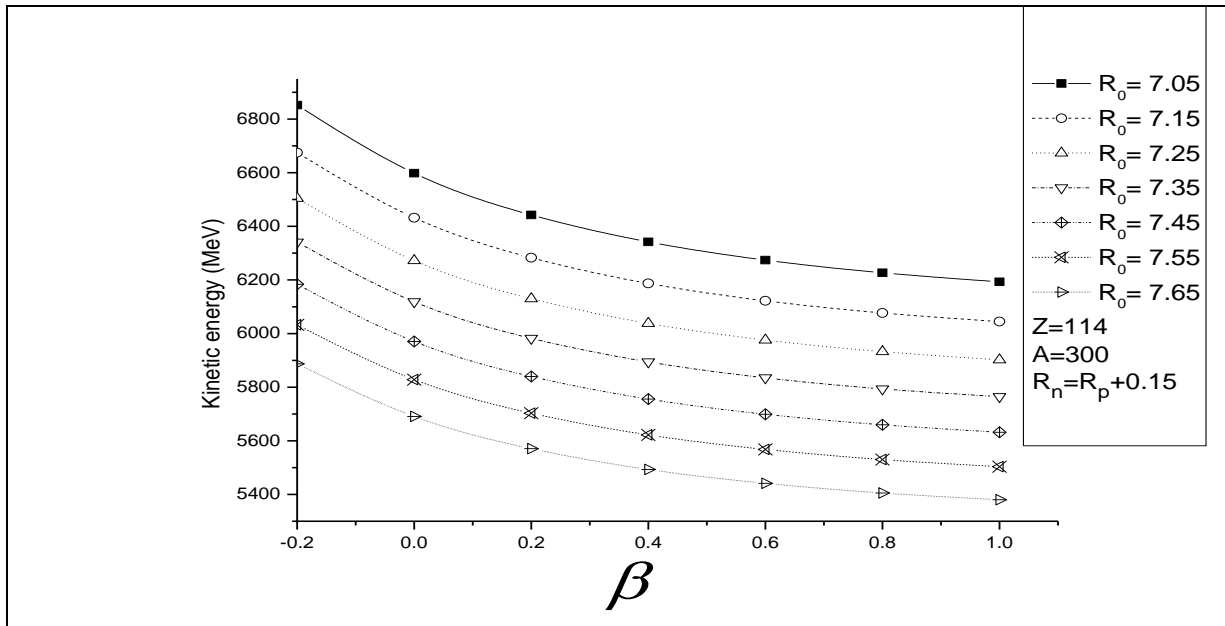
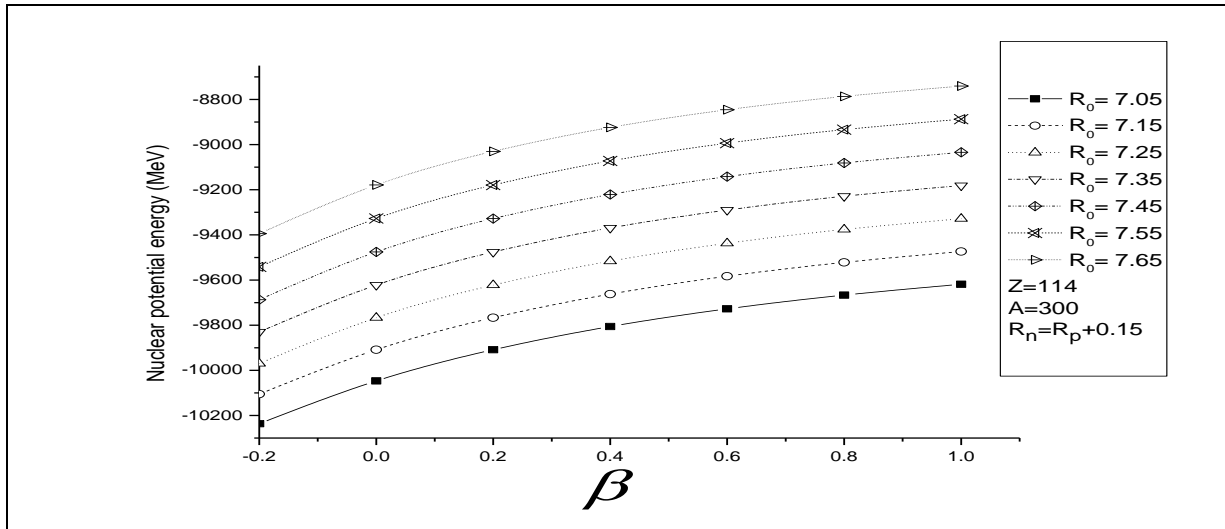


Figure 3(b): The variation of the kinetic energy with depression parameter  $\beta$  for <sup>300</sup>Fl nucleus.



Figure(3c): The variation of potential energy of  $^{300}\text{Fl}$  nucleus with depression parameter  $\beta$ .

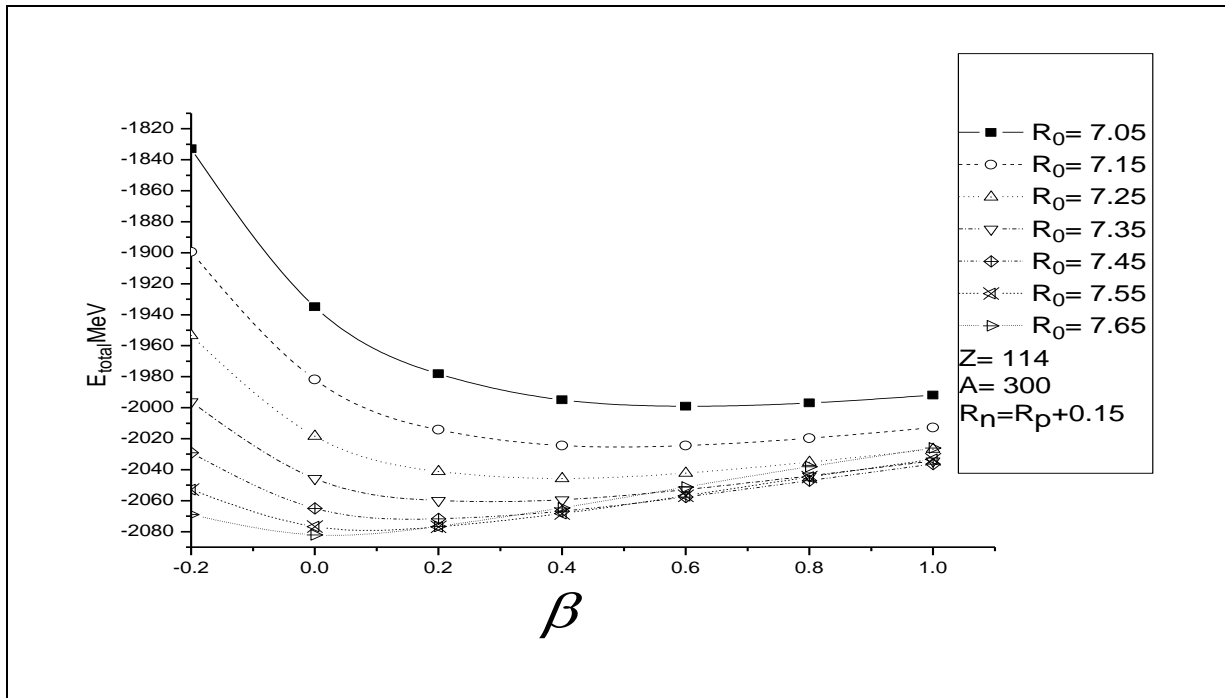


Figure 3(d): The variation of the total energy (sum of the kinetic, nuclear and Coulomb energies) of SHE  $^{300}\text{Fl}$ , without shell and pairing energy corrections, with depression parameter  $\beta$ .

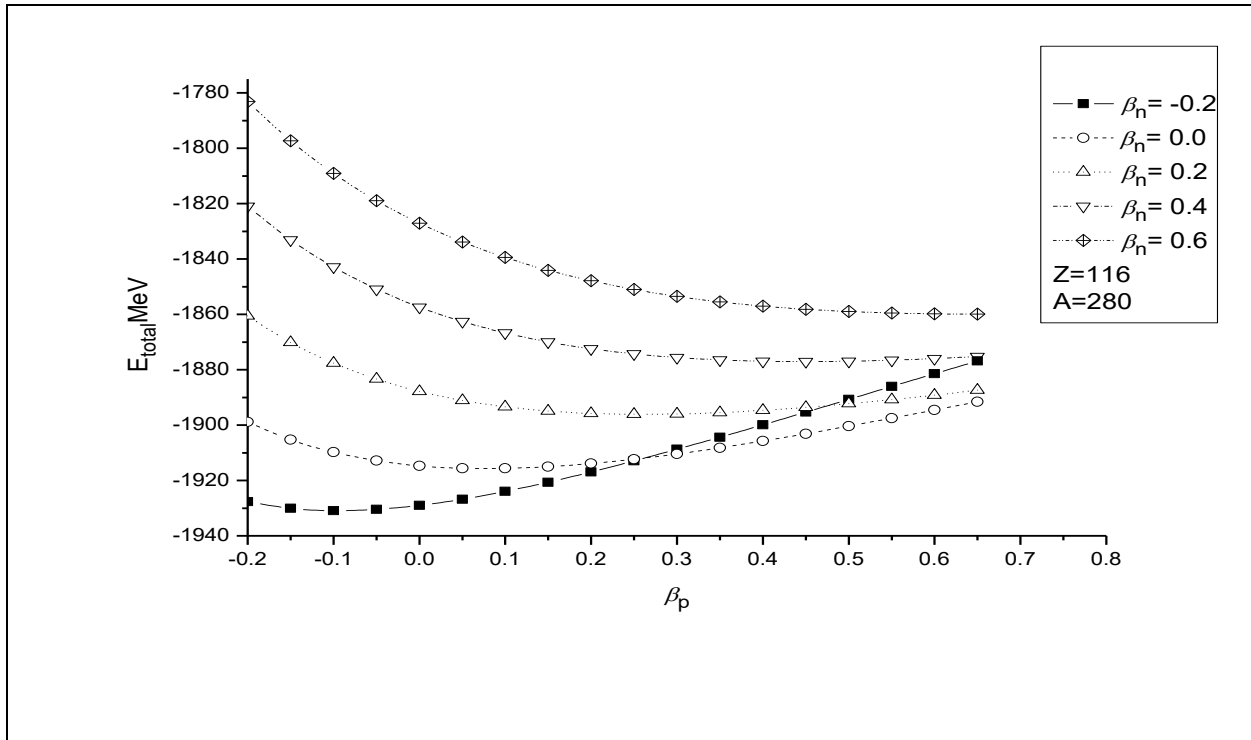
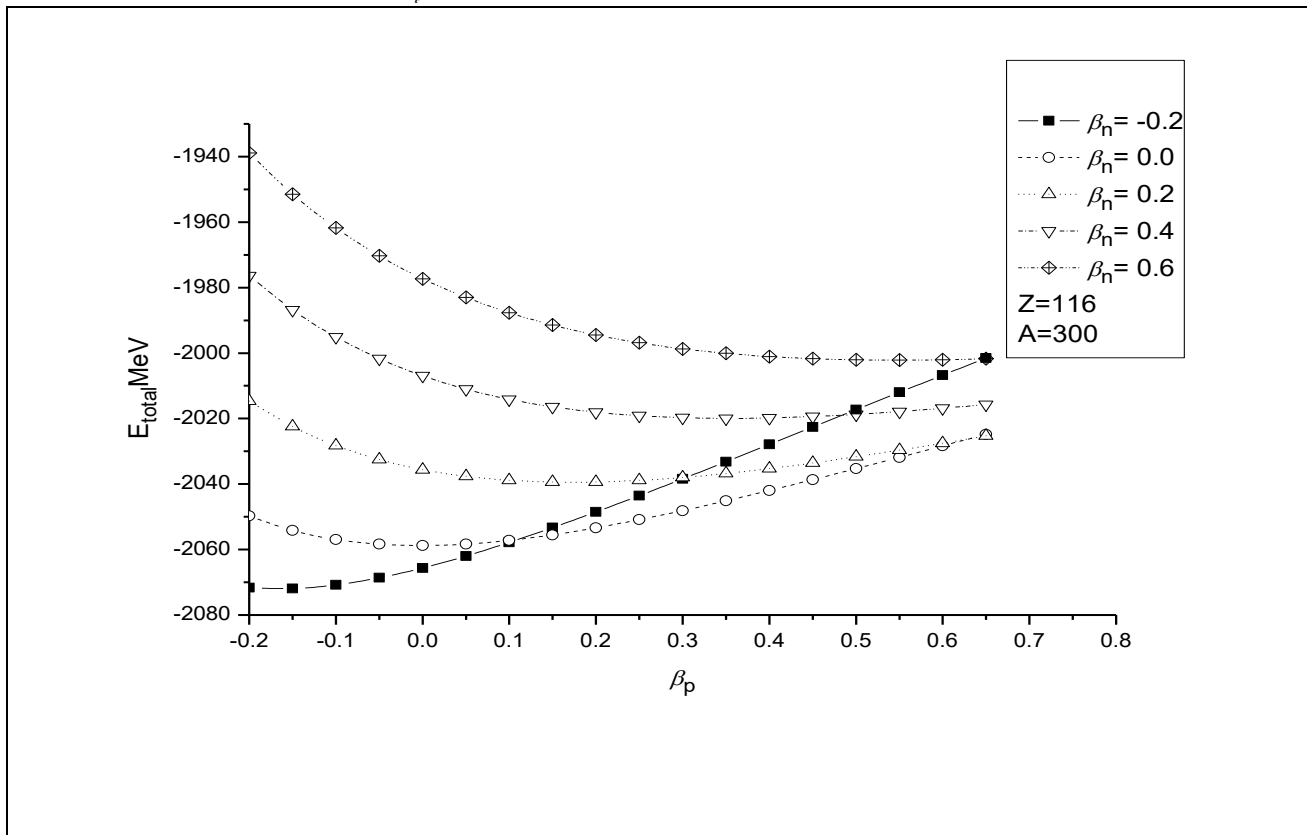


Figure (4a): The variation of the total energy (sum of the kinetic, nuclear and Coulomb energies) of SHE  $^{280}_{116}$  without shell and pairing energy corrections, with proton depression parameter  $\beta_p$ .





**Figure (4b):** is the same as Figure (4a), but for the SHE  $^{300}_{116}$ .

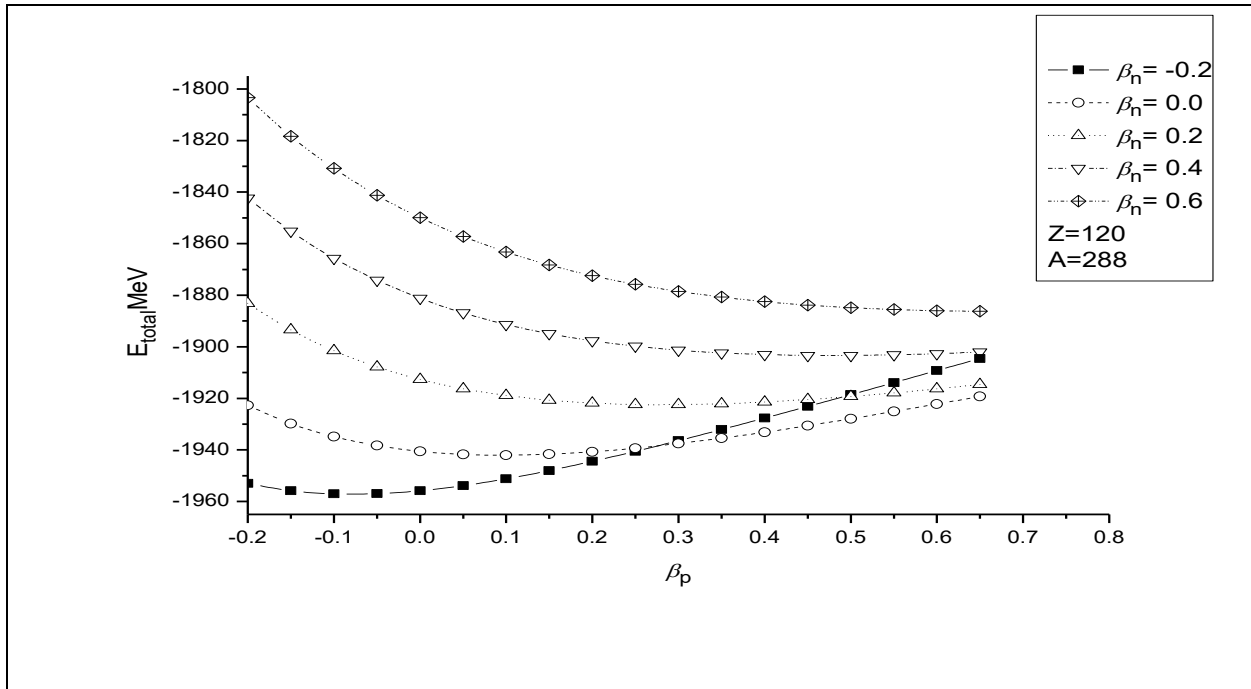


Figure (5a): Is the same as Fig. (4a), but for the SHE  $^{288}_{120}$ .

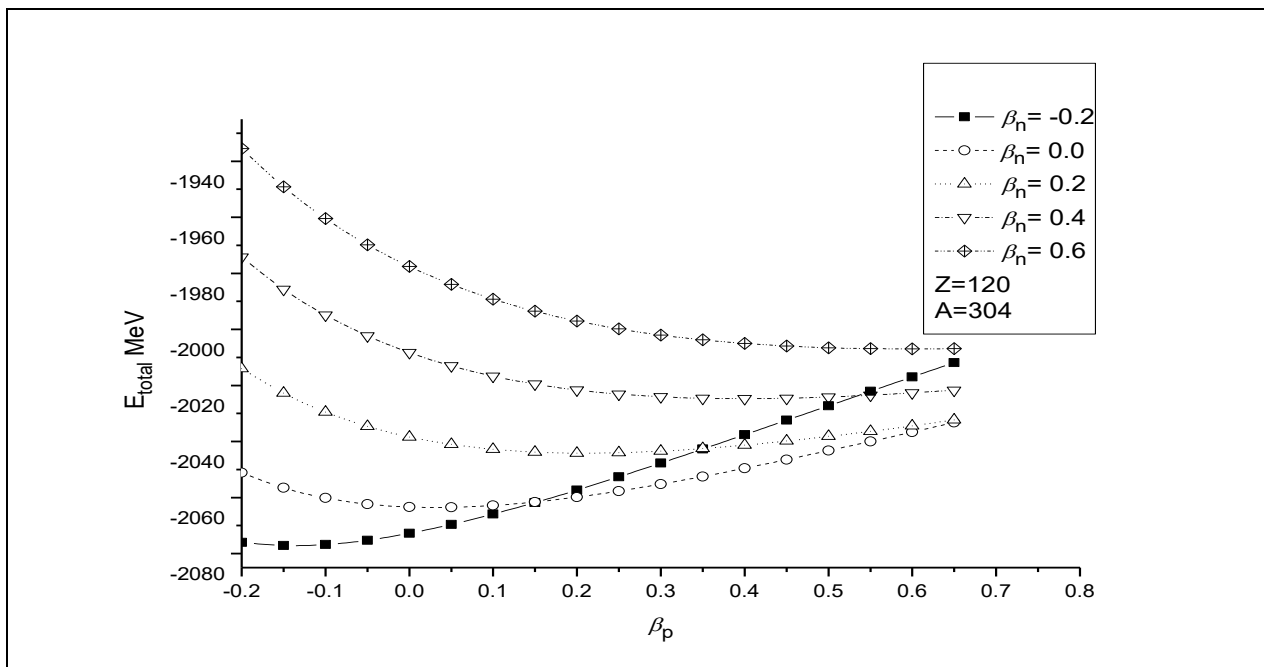




Figure (5b): is the same as Fig. (4a), but for the SHE  $^{304}120$ .

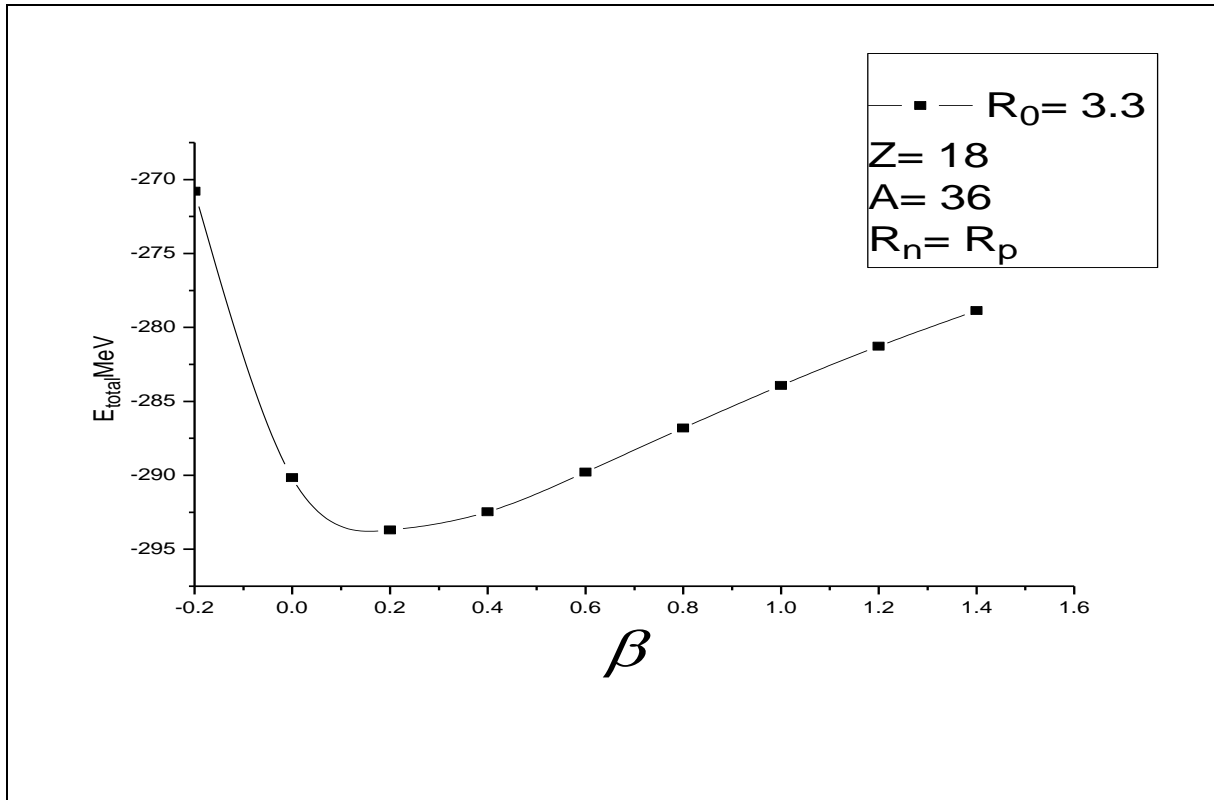


Figure (6a): The variation of the total energy (sum of the kinetic, the nuclear and the Coulomb energies) of the  $^{36}_{18}\text{Ar}$  nucleus, without shell and pairing energy corrections, with depression parameter  $\beta$ .

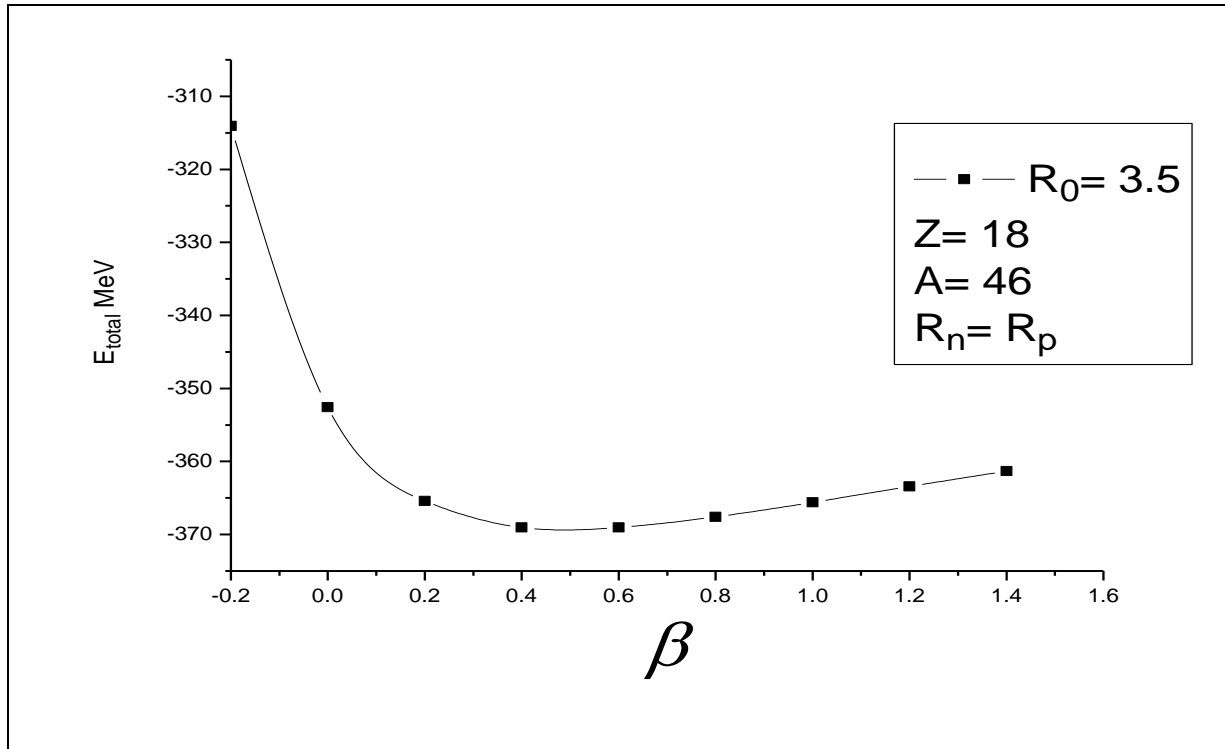


Figure (6b): is the same as Fig. (6a), but for the  ${}^{46}_{18}\text{Ar}$  nucleus.

## REFERENCES

- [1] Oganessian, Yu. Ts. Utyonkov, V. K. Lobanov, Yu. V. et al., Phys. Rev. C (2009), Attempt to produce element 120 in the Pu244+Fe58 reaction, 79, 024603.
- [2] Chu, Y., Wang, Z. and Dong, T. Phys. Rev. C (2010), Central depression of nuclear charge density distribution 82, 024320., and Afanasjev, A. V. and Frauendorf, S., Phys. Rev. C (2005), Central depression in nuclear density and its consequences for the shell structure of superheavy nuclei, 71, 024308.
- [3] Grasso, M., et al Phys. Rev. C (2009), nuclear "bubble" structure in Si34, 79, 034318.
- [4] Ismail, M., et al, Phys Rev. C (2005) Orientation dependence of the heavy-ion potential between two deformed nuclei, 72 064616,
- [5] Barrel, J., Bencheikh, K., Eur. Phys. J A (2002) Nuclear mean fields through self-consistent semiclassical calculations, 14, 179.
- [6] Denisov, V. Yu. and Nesterov, V. A. Phys. At. Nucl. (2002), Binding Energies of Nuclei and Their Density Distributions in a Nonlocal Extended Thomas-Fermi Approximation, 65, 814.
- [7] De Jager, C. W., De Vries, H. and De Vries, C. At. Data Nucl. Data Tables (1974) 14, 479.
- [8] Ismail, M., et al Phys. Atomic Nuclei (2010) Systematics of  $\alpha$ -decay half-lives around shell closures 73, 10.
- [9] Beiner, M., et al Nuclear Phys. A (1975), Nuclear ground-state properties and self-consistent calculations with the Skyrme interaction: (I). Spherical description, 238, 29.
- [10] Bartel, J., et al Nuclear Phys. A (1982), Towards a better parametrisation of Skyrme-like effective forces: A critical study of the SkM force, 386, 79.
- [11] Dobaczewski, J., Flocard H., Treiner, J. Nuclear Phys. A (1984), Hartree-Fock-Bogolyubov description of nuclei near the neutron-drip line, 422, 103

[12] Chabanat, E., et al Nuclear Phys. A (1998), A Skyrme parametrization from sub nuclear to neutron star densities Part II. Nuclei far from stabilities, 635-231.